An Axial Dispersion Model of Competing Ion Etching and Mixing of Binary Solids

Raul J. Elias and Mark A. Barteau
Dept. of Chemical Engineering, University of Delaware, Newark, DE 19716

Ion bombardment of solid surfaces produces a number of changes in the near-surface region. The surface is etched by ejection of material by momentum exchange. The surface concentrations of the components of a multicomponent solid, such as an alloy, are altered by preferential sputtering. Finally, the incident ions penetrate a distance into the solid, producing a damaged region referred to as the "altered layer" in which diffusion is enhanced relative to that in the unaltered bulk. Previous models have not explicitly accounted for the ion penetration depth and the discontinuity of solid diffusivities at this boundary. We demonstrate that this problem is directly analogous to that of a plug-flow reactor with axial dispersion, and solve for steady-state and transient concentration profiles in a binary solid, taking into account the different values of the "Peclet number" appropriate for the two regions, the altered layer and the unaltered bulk of the solid.

Introduction

The properties of a solid, and in particular those of the near-surface region, can be affected greatly by radiation. Understanding the role of solid surfaces is crucial in many technologies; ion beam processes provide tools to characterize solids and to modify surface properties. Indeed, the use of ions for sputtering to remove or implant materials has reached manufacturing process status.

Sputtering has been found to eject surface atoms of compound targets nonstoichiometrically; this phenomenon is known as preferential sputtering. By varying the sputtering parameters, alloys can generally be sputtered to a wide range of surface compositions. In addition to removal of material from a surface, sputtering may be utilized to apply material to a surface. Specific applications of sputtering from a target onto a surface of interest include preparation of alloys, application of refractory materials, and fabrication of microcircuit metallization layers, oxide microcircuit oxidation layers, transparent conducting electrodes, amorphous optical films for integrated optics devices, piezoelectric transducers, photoconductors and luminescent films for display devices, thin film resistors and capacitors, video-discs, solid electrolytes, thin film lasers, and microcircuit photolithographic mask blanks (Thornton, 1983).

Ion bombardment at moderate energies (in the kilovolt range) is typically carried out at pressures in the range from 5×10^{-4} to 5×10^{-7} Torr (Thornton, 1983). The sample is bombarded and eroded by energetic particles, usually ions of a heavy inert gas. Material is dislodged and ejected from the surface by momentum exchange. The sputtered material is ejected primarily in atomic form (Betz and Wehner, 1983; Thornton, 1983). In addition to ejecting material from the surface, the impinging ions penetrate a distance λ into the solid, creating rough morphological changes at the surface and atomic mixing within a comparable depth beneath the surface. The penetration depth of the ions depends on the energy and atomic mass of the ions as well as on the atomic masses of the solid components (Ryssel and Ruge, 1986). Simple models based on collisional processes alone can be used to calculate the number and distribution of atoms displaced by impinging ions (Schiøtt, 1970); however, more complex models are needed to determine the structural damaged caused by the beam (Williams and Poate, 1984).

Preferential sputtering of different atoms from the surface is also a function of mass differences of the atoms in multicomponent systems such as alloys. Surface binding energy differences or chemical bonding differences between the atoms, the location of the atoms themselves at or near the surface, and recoil implantation or cascade mixing have also been proposed to contribute to the effects of preferential sputtering in alloys (Pickering, 1976; Ho et al., 1976; Betz and Wehner,

Correspondence concerning this article should be addressed to M. A. Barteau.

1982; Swartzfager et al., 1982; Ossi, 1987), and are difficult to predict *a priori*. Chemical reactions between the ion beam and the components of the solid can be neglected for the case of bombardment with noble gas ions considered here, but will also contribute to the distribution of components in the solid in the case of reactive ion etching.

Preferential sputtering of solid components by ions of an inert gas is typically represented as a first-order kinetic process (Ho et al., 1976; Ho, 1978). As a semi-infinite binary alloy is continuously bombarded by ions, the surface will become depleted of the easy-to-sputter component. Since there is then less and less of this component to sputter, its rate of removal will decrease. At steady state, relative rates of removal of the two components must match the ratio of their bulk concentrations, that is, there is no further change of the relative concentrations with time. This situation is achieved when the surface concentration ratio has been adjusted by sputtering to compensate exactly for the different cross sections for sputtering (that is, different rate constants for removal) of the two components.

In a semi-infinite binary alloy, preferential sputtering of one component from the surface will give rise to a concentration gradient within the near-surface region. The thickness of the "altered layer," the region in which the concentration deviates from the bulk concentration, is typically taken to be comparable to the ion penetration depth itself (Ho et al., 1976; Swartzfager et al., 1982; Ossi, 1987; Peng et al., 1987). Experimental evidence for an "altered layer" can be found in a number of studies. Gillam (1959) and Laegried and Wehner (1961) bombarded binary alloys with inert gas ions and examined the corresponding electron diffraction patterns. They observed distinct doublets in the diffraction patterns, indicating the formation of an altered layer near the surface with lattice parameters and thus composition different from those of the original alloy. MacDonald and Haneman (1966), Tarng and Wehner (1971), and Quinto et al. (1971) later reported similar findings. MacDonald and Haneman (1966) also attempted to measure the depth of the altered layer. It is the concentration profiles within and beyond the "altered layer" which are of interest here in examining the effects of ion bombardment.

The atomic mixing created by ion bombardment can be represented as an enhancement of diffusion within the altered layer, that is, an increase in the binary diffusion coefficient. It has been estimated, for example, that this altered layer has an ion-bombardment-enhanced diffusion coefficient of approximately 10^{-16} cm^2/sec to 10^{-17} cm^2/sec in Cu-Ni, Au-Pd, and Ag-Au alloy systems (Pickering, 1976; Swartzfager et al., 1982), with an incident beam of 2.0 keV, ^{20}Ne as the probe ion, and a current density of 2.5 μA/cm^2. Values for unenhanced diffusion coefficients are of order 10^{-18} cm^2/sec similar to those for self-diffusion in metals (Birchenall, 1959; Girifalco, 1964). Thus two distinct diffusion regions are created in the sputtered alloy: an enhanced diffusion region (altered layer) in which diffusion coefficients may be increased by several orders of magnitude and an unaffected diffusion region in the bulk.

As the surface is bombarded initially, preferential sputtering will give rise to a concentration gradient via depletion of the more-easily-sputtered component at the surface. Within the solid, the concentration profile is determined by the local diffusive properties of the alloy. The concentration of the more-easily-sputtered component will be a minimum at the surface under steady-state conditions. The concentration of this component will increase as one moves into the bulk toward the boundary between the two diffusion regions. The rate of increase will depend on the ratio of the sputtering rate to the diffusion rate. At the internal interface between the two diffusion regions, the concentration must be a continuous function; however, there will be a discontinuity in the concentration gradient because of the difference in diffusion coefficients on opposite sides of the interface. As the concentration profile is followed into the unaltered bulk, it is expected to increase sharply, since the diffusion coefficient is much smaller, but the rate of transport to the surface must be constant at steady state. At large distances from the surface, the concentration approaches that of the bulk. We demonstrate below that this problem is directly analogous to the problem of a plug-flow reactor (PFR) with axial dispersion (Danckwerts, 1953; Wehner and Wilhelm, 1956; Pearson, 1959; Bischoff, 1961; van Cauwenberghe, 1966), and that the competition between etching and mixing processes can be accounted for by a dimensionless quantity analogous to the Peclet number.

Previous Models of Preferential Sputtering Effects

Pickering (1976) modeled the effects of preferential sputtering by Fick's law. The binary alloy was assumed to consist of an easy-to-sputter and a difficult-to-sputter material; however, no quantitative description of the preferential sputtering dynamics was given. The mole fraction, C, of the easy-to-sputter material was set equal to zero at the surface. He obtained for the concentration profile

$$C = C_B\left\{1 - 0.5e^{\frac{-ux-u^2t}{D}} \cdot \operatorname{erfc}\left[\frac{x}{2D^{0.5}t^{0.5}} - \frac{ut^{0.5}}{D^{0.5}}\right] - 0.5\operatorname{erfc}\left[\frac{x}{2D^{0.5}t^{0.5}}\right]\right\} \quad (1)$$

where C_B is the bulk mole fraction of the easy-to-sputter component, D is the Fickian diffusion coefficient, u is the rate of recession of the surface (assumed to be constant), x is the distance from the surface into the solid, and t is the time. He then estimated the effective thickness of the altered layer to be

$$\lambda \approx \frac{C|_{x=0}}{\left.\frac{\partial C}{\partial x}\right|_{x=0}} \approx \frac{D}{u} \quad (2)$$

This estimate of the altered layer thickness arbitrarily equates the rate of sputtering with the rate of diffusive transport; that is, it is not directly related to the actual penetration depth of the incident ions.

Ho et al. (1976) took into account the different sputter yields of different components in defining the surface condition, and set up mass balances for the altered layer taking into account both removal of material from the surface and diffusion from the bulk. Ho (1978) produced a solution for the concentration profile in alloy etching, applying the kinetic model for pref-

erential sputtering of Ho et al. (1976). Unfortunately, the effects of enhanced diffusion were assumed throughout the entire alloy; only one diffusion region was defined. Ho obtained

$$C = C_B - \frac{C_B}{2}\left[\operatorname{erfc}\left(\frac{X+T}{2T^{0.5}}\right) + \frac{H}{H-1}e^{-X}\operatorname{erfc}\left(\frac{X-T}{2T^{0.5}}\right)\right] + \frac{C_B(2H-1)}{2(H-1)}e^{HX+H(H-1)T}\operatorname{erfc}\left(\frac{X-(2H-1)T}{2T^{0.5}}\right) \quad (3)$$

where

$$X = \frac{ux}{D} \quad (4)$$

$$T = \frac{u^2 t}{D} \quad (5)$$

Ho (1978) defined the kinetic factor, H as follows

$$H = \frac{(S_Q - S_P)[1 - C_S]}{S_P C_S + S_Q[1 - C_S]} \quad (6)$$

where C_S is the surface mole fraction of P at time t and S_P and S_Q represent the sputtering rates of the respective components. In determining the concentration profile, Eq. 3, H was assumed to be a constant and was evaluated at steady state:

$$H = 1 - \frac{C_B}{C_{S,SS}} \quad (7)$$

Ho estimated

$$\frac{u\lambda}{D} \approx 1 \quad (8)$$

or

$$\lambda = \frac{D}{u} \quad (9)$$

as did Pickering (1976), arbitrarily assuming that the rate of removal of material from the surface by sputtering is equal to the rate of diffusive transport. This condition may appear to be a definition of steady state; however, it is not. Because the surface is moving, there is also a "convective" term in the steady-state mass balance.

Swartzfager et al. (1982) improved this model by allowing for uphill diffusion, diffusion against a concentration gradient caused by preferential sputtering. The diffusion flux was expressed in terms of jump probability frequencies, however, the diffusion coefficient was kept constant throughout the entire solid, defining again only one diffusion region.

Peng et al. (1987) modeled sputtering in binary films of finite thickness on top of a single component bulk and fitted some experimental data. They obtained

$$C(t) = C_\delta\left[1 - \left(\frac{ut}{\delta}\right)\right]^{\frac{u_P - u}{u}} \quad (10)$$

where $C(t)$ is the average mole fraction of component P in the film, C_δ is the initial fraction of P in the film, u_P is the sputtering rate of component P, u is the total sputtering rate, and δ is the initial thickness of the binary film. The concentration model was then convoluted with the sampling function for Auger Electron Spectroscopy to obtain the time dependence of the Auger signal for P. The data fits were good for sputtering through films with thicknesses of order 30–40 Å. However, the interior boundary of the enhanced diffusion region was fixed for all time at the initial film boundary, thus this model cannot account for inward diffusion when the altered layer boundary passes the original film boundary.

The aim of the present work was to develop a more rigorous model of the effects of enhanced diffusion under ion bombardment. There are two major differences between the previous models and that proposed here. The first difference is that this model assumes that the incident ions, penetrating a finite distance into the alloy, create a diffusion interface at λ. The presence of this interface creates two distinct diffusion regions: at distances from the surface less than λ the diffusion coefficient, D_1, is assumed to be constant but enhanced; at distances greater than λ the diffusion coefficient, D_2, is characteristic of that in the unperturbed bulk alloy. It has been estimated that $D_1 \approx \beta D_2$, where β is a value in the range of 10 to 100 or greater (Pickering, 1976; Swartzfager et al., 1982; Borg and Dienes, 1988). Our reanalysis of the Peng et al. (1987) data for sputtering of magnesium nitride films with 1 keV argon ions suggests that for this case β is approximately 20 and the ratio of etching to diffusion rates for the altered layer is of order unity (Elias, 1990). The parameters used in the model calculations below were therefore chosen to span a range which included these values. Neglect of the 1 to 2 order of magnitude difference in diffusivities in the altered layer and the bulk, as in previous models, can lead to 50 to 100% errors in the predicted signal intensities for spectroscopic techniques, for example, Auger Electron Spectroscopy, used to monitor surface concentrations (Elias, 1990).

The second difference between this and previous models is that this work does not assume that the rate of sputtering will be equal to the rate of diffusive transport within the alloy. In past studies, the convective to diffusive transport ratio has been set equal to 1 or 0 arbitrarily, and λ has not entered explicitly into the model. However, in the present model, the ratio of convective to diffusive transport is not fixed arbitrarily. λ is set equal to the ion penetration depth and appears explicitly in the model. The ion penetration limit, λ, is assumed to be a single value rather than its actual Gaussian distribution (Mintz et al., 1985). The half-width of the ion range distribution has been calculated to be approximately 0.1 λ over a wide range of beam/solid atomic mass ratios (Schiøtt, 1970). The distribution of penetration depths of the incident ions is neglected in the analysis that follows; inclusion of such effects would be expected to reduce but not eliminate the sharp discontinuities in the concentration profiles predicted.

Model Development

If one assumes a sputtering rate which is first-order in surface concentration, the rates at which components P and Q leave the surface can be expressed as

$$\frac{dN_P}{dt} = k_P C_{S,P} \rho \tag{11}$$

and

$$\frac{dN_Q}{dt} = k_Q C_{S,Q} \rho \tag{12}$$

where N_i is the number of moles of species i, ρ is the molar density of the solid (assumed to be independent of composition), k_i is the rate constant for the ejection of i from the surface, $C_{S,i}$ is the surface mole fraction of component i, and the subscript i refers to either component P or Q. Equations 11 and 12 assume that the rate of loss of i from the surface is a linear function of the surface concentration for that component (Ho et al., 1976; Ho, 1978).

The ratio of removal rates, defined as the selectivity of sputtering, is obtained by dividing Eqs. 11 by 12:

$$\frac{dN_P}{dN_Q} = \frac{k_P}{k_Q}\frac{C_{S,P}}{C_{S,Q}} = \frac{k_P C_{S,P}}{k_Q(1 - C_{S,P})} \tag{13}$$

The concentration ratio of the material in the bulk must equal the selectivity for removal from the surface at steady state. In the analysis that follows, only component P, the more easily sputtered component, will be treated; the subscript will be dropped.

Therefore, at steady state

$$\frac{\kappa C_{S,SS}}{1 - C_{S,SS}} = \frac{C_B}{1 - C_B} \tag{14}$$

where SS denotes values at steady state and

$$\kappa = \frac{k_P}{k_Q} \tag{15}$$

where κ is defined to be greater than 1.

Equation 14 is now solved for C_B to obtain

$$C_B = \frac{\kappa C_{S,SS}}{1 - C_{S,SS} + \kappa C_{S,SS}} \tag{16}$$

$$C_{S,SS} = \frac{C_B}{\kappa + C_B - \kappa C_B} \tag{17}$$

Therefore the kinetic factor of Ho (1978) from Eq. 7 can be expressed in terms of κ and C_B only:

$$H = (1 - \kappa)(1 - C_B) \tag{18}$$

If one assumes a constant diffusion coefficient in the altered layer, a constant diffusion coefficient in the unaltered bulk, and a constant density throughout the entire alloy, a mass balance for a differential slice of the alloy yields

$$D_j \frac{\partial^2 C}{\partial x^2} + v\frac{\partial C}{\partial x} = \frac{\partial C}{\partial t} \tag{19}$$

where $v = -u$ and where the subscript j refers to region 1 (the altered layer) or region 2 (the bulk), depending on the location at the differential element.

In solving Eq. 19, two boundary conditions would normally be needed. In this case, the domain is divided into two diffusion regions, and each region has a characteristic D_j. The problem posed here is then of two differential equations of the form of Eq. 19: one holds for $0 \le x \le \lambda$ with D_1 and the other holds for $x > \lambda$ with D_2. Thus four boundary conditions are needed.

The first boundary conditions is that of Ho (1978), obtained from a balance of the mass flux at the outer surface, that is, at the solid-vacuum interface. For $t > 0$ and $x = 0$ this yields

$$D_j \frac{\partial C_S}{\partial x} + Hv C_S = 0 \tag{20}$$

The second boundary condition is provided by the requirement that the concentrations on both sides of the diffusion interface match. For $t > 0$ and $x = \lambda$, this yields

$$C|_{\lambda-} = C|_{\lambda+} \tag{21}$$

where the subscript $\lambda-$ refers to the interface on the altered layer side, and the subscript $\lambda+$ refers to the interface on the bulk side.

The third boundary condition is obtained from a mass balance at the diffusion interface. Since diffusion does occur at $x = \lambda$, $C|_\lambda \neq C_B$, and a mass balance at this interface is therefore also required. For $t > 0$ and $x = \lambda$, this yields

$$D_1 \left.\frac{\partial C}{\partial x}\right|_{\lambda-} + vC|_{\lambda-} = D_2 \left.\frac{\partial C}{\partial x}\right|_{\lambda+} + vC|_{\lambda+} \tag{22}$$

Equation 22 is essentially equivalent to the Danckwerts boundary condition for the entrance region of a PFR with axial dispersion.

The fourth boundary condition is provided by the condition at infinity. For $t > 0$ and as $x \to \infty$

$$C = C_B \tag{23}$$

The initial condition is then the following. At $t = 0$,

$$C = C_B \tag{24}$$

for all $x \ge 0$.

Equations 19–24 are then nondimensionalized with

$$z = \frac{x}{\lambda} \tag{25}$$

$$\tau = \frac{vt}{\lambda} \tag{26}$$

and

$$\pi = \frac{C}{C_B} \tag{27}$$

The resulting nondimensional characteristic equation is

$$\frac{1}{Pe_j}\frac{\partial^2\pi}{\partial z^2}+\frac{\partial\pi}{\partial z}=\frac{\partial\pi}{\partial\tau} \tag{28}$$

The appropriate boundary, matching, and initial conditions become the following.

Boundary Condition 1: At $t>0$ and $z=0$

$$\frac{1}{Pe_1}\frac{\partial\pi}{\partial z}+H\pi=0 \tag{29}$$

Boundary Condition 2: At $t>0$ and $z=1$

$$\pi|_{1-}=\pi|_{1+} \tag{30}$$

Boundary Condition 3: At $t>0$ and as $z=1$

$$\frac{1}{Pe_1}\frac{\partial\pi}{\partial z}\bigg|_{1-}+\pi|_{1-}=\frac{1}{Pe_2}\frac{\partial\pi}{\partial z}\bigg|_{1+}+\pi|_{1+} \tag{31}$$

Boundary Condition 4: At $t>0$ and $z\to\infty$

$$\pi=1 \tag{32}$$

Initial Condition: At $t=0$ for all z

$$\pi=1 \tag{33}$$

It is interesting to note the emergence of a parameter—the etching rate to diffusion rate ratio—represented here as the Peclet number, which is analogous to the Peclet number for 1 – dimensional axial dispersion in a plug-flow reactor.

$$Pe_j\equiv\frac{v\lambda}{D_j} \tag{34}$$

where $j=1$ or 2, depending on which region of the alloy, the altered layer or the unaltered bulk, for which the mass balance is constructed. Placing the Peclet number in the context of this problem, it can be said that ion bombardment defines the alloy into two distinct transport regions, or into two distinct Peclet number regions: a low Pe region, in the altered layer and a high Pe region in the bulk of the solid. Strictly speaking, the value of Pe_1 is time-dependent, as the altered layer does not exist prior to ion bombardment, but requires a finite ion dose (and therefore a finite time) for the diffusion coefficient in this region to reach its radiation-enhanced value. The altered layer is generally considered to be fully established when a sufficient number of ions have penetrated the solid so that their collision cascades (the damaged regions surrounding each ion track) overlap to fill the entire layer (Davies, 1992). Experimental and theoretical determinations both demonstrate that this process is quite rapid, occurring at ion fluences comparable to the atom density of the exposed surface (Ossi, 1987; Davies, 1992; Picraux et al., 1992). Thus the timescale for establishment of the altered layer is less than that for removal of a single layer of atoms from the surface, and can therefore be neglected for all but the thinnest films. In the model developed here, the values of D_1, D_2, Pe_1, and Pe_2 are assumed to be time-invariant; that is, diffusion in the altered layer is enhanced relative to its value in the bulk for all $t>0$.

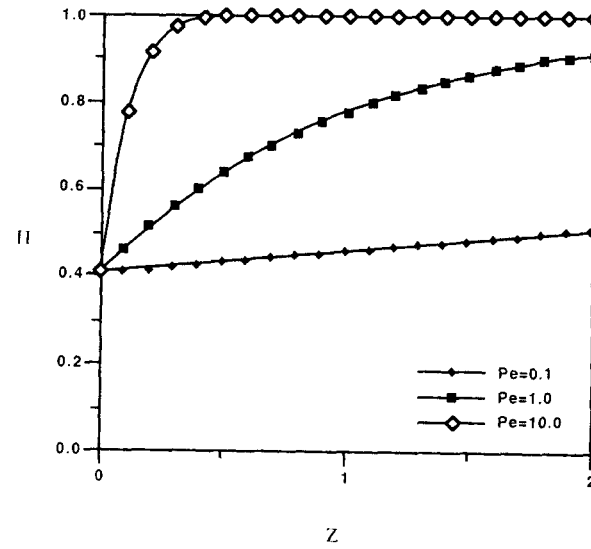

Figure 1. Steady-state profiles for varying Pe, $Pe_1 = Pe_2$.
$C_B = 0.5$ and $\kappa = 4.0$.

Steady-State Solution

At steady state, Eq. 28 reduces to

$$\frac{1}{Pe_j}\frac{\partial^2\pi}{\partial z^2}+\frac{\partial\pi}{\partial z}=0 \tag{35}$$

The boundary conditions, Eqs. 29–32 are unchanged.

If one assumes a constant Pe throughout the alloy, that is $Pe_1=Pe_2=Pe$, there is no unique value for λ, the ion penetration depth. λ cancels out of the boundary conditions at the interface. Equations 30 and 31 become identities.

Equation 35 can now be solved analytically subject to the boundary conditions:

$$\pi(z)=1-\frac{H}{H-1}e^{-zPe} \tag{36}$$

This is equivalent to the solution of Ho (1978) at steady state with $Pe=1$. The steady-state solution for $Pe_1\neq Pe_2$, where $Pe_1<Pe_2$ is also straightforward. In this case, the boundary at $x=\lambda(z=1)$ divides the two diffusion regions.

$$\pi(z)=\begin{cases}1-\dfrac{H}{H-1}e^{-zPe_1}, & \text{Region 1: } 0\le z\le 1;\\[2ex] 1-\dfrac{H}{H-1}e^{-Pe_1-Pe_2(z-1)}, & \text{Region 2: } z>1\end{cases} \tag{37}$$

Representative illustrations of the steady-state concentration profiles are shown in Figures 1–3. In Figure 1, a plot of π vs. z from Eq. 36 is shown for different values of Pe, with $C_B=0.5$ and $\kappa=4.0$ chosen as representative values. The concentration increases concave down with z. The $Pe=.10$ curve is relatively flat, similar to that of a flow reactor of the same Pe. The

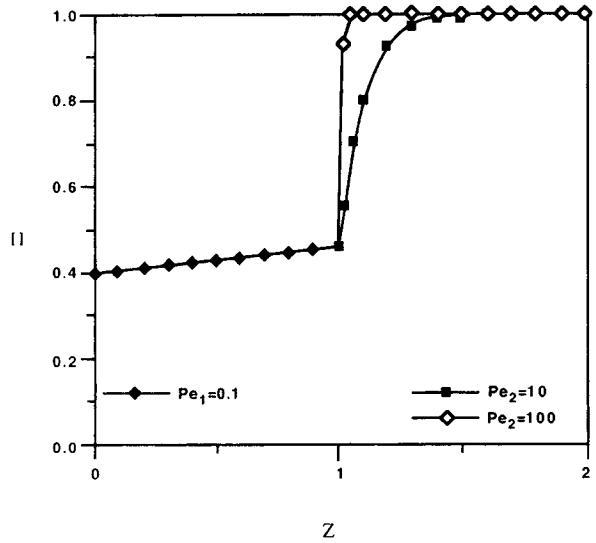

Figure 2. Steady-state profile for $Pe_1 = 0.1$ and for $Pe_2 = 10.0$ and $Pe_2 = 100.0$.

$C_B = 0.5$ and $\kappa = 4.0$.

$Pe = 1.0$ profile is intermediate in curvature, similar to that of an intermediate case between a continuously stirred tank reactor (CSTR) and a PFR with no reaction. The $Pe = 10.0$ curve exhibits a very sharply increasing concentration profile, similar to that of a PFR with no reaction.

For the case of $Pe_1 = Pe_2 = Pe = 1.0$, the above solution reduces to the steady-state solution obtained by Ho (1978). By assuming $Pe_1 = Pe_2 = Pe$, the enhanced diffusion properties are extended infinitely into the bulk, or conversely, there is no radiation enhancement of diffusion. There is no reason to believe that the enhanced diffusion will be a property of the entire alloy, since the ion beam which is presumed to enhance diffusion only penetrates a finite distance into the solid.

Figures 2 and 3 illustrate the steady-state solutions given by Eq. 37 for $C_B = 0.5$ and $\kappa = 4.0$. $Pe_1 = 0.1$ and $Pe_1 = 1.0$ characterize the enhanced diffusion region and $Pe_2 = 10.0$ and $Pe_2 = 100.0$ are both used in each case. For higher values of Pe_1, that is, $Pe_1 \geq 10$, the solutions are essentially indistinguishable from those where $Pe_1 = Pe_2$.

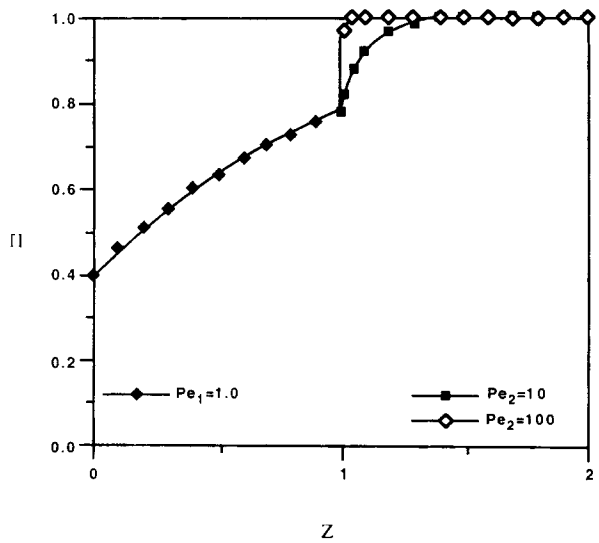

Figure 3. Steady-state profile for $Pe_1 = 1.0$ and for $Pe_2 = 10.0$ and $Pe_2 = 100.0$.

$C_B = 0.5$ and $\kappa = 4.0$.

In Figure 2, the concentration profile is relatively flat in region 1, characteristic of a low Pe. In region 2, the concentration profile jumps to very high values within a very short distance into the unaltered bulk, characteristic of high Pe. The $Pe_2 = 100.0$ curve shows a faster concentration increase than the $Pe_2 = 10.0$ curve in reaching the bulk concentration, as expected.

In Figure 3, the concentration profile increases over the entire region 1, characteristic of an intermediate value of Pe. In region 2, the concentration also jumps to very high values within a very short distance of the interface, characteristic of a high Pe. The $Pe_2 = 100.0$ curve shows a faster approach to the bulk composition than the $Pe_2 = 10.0$ curve, as expected.

The most notable characteristic of these profiles is the sharp concentration gradient discontinuity at the diffusion interface between region 1 and region 2. The greater the difference between Pe_1 and Pe_2, the greater is the discontinuity in the slope of the concentration profile at the interface. If $Pe_1 = Pe_2$, Eq. 37 reduces to Eq. 36—the distinction into regions with different Pe becomes meaningless. The greater Pe_2, the smaller is the distance past the interface required for the concentration to reach C_B.

In addition, the shape of the profile in region 1 is unaffected by Pe_2. If a closer inspection of boundary condition 3 is made, an explanation is found. In changing Pe_2 from 10.0 to 100.0, the third term of Eq. 31

$$\frac{1}{Pe_2}\frac{\partial \pi}{\partial z}\bigg|_{1+}$$

is the only term affected. In effect, this term represents a dimensionless diffusive flux: it is first divided by 10.0 and then by 100.0. The effect of this diffusive flux on the boundary condition for $Pe_1 \leq 0.10$ Pe_2 is minimal. Only when Pe_2 approaches Pe_1 does this term become an important factor in the boundary condition, and hence the solution of the profiles.

Transient Evolution of the Concentration Profile Under Ion Bombardment

The next stage is to find the transient solution of Eq. 28 in an alloy of semi-infinite thickness. In this stage, transient profiles are obtained which should approach the steady-state solutions above for $C_B = 0.5$ and $\kappa = 4.0$, for the corresponding values of Pe_1 and Pe_2. Again, the domain must be split into two regions, $0 \leq z \leq 1$ and $z > 1$, with the appropriate Pe_j for each region. Due to the complexity of Eq. 28 and the associated boundary conditions, a numerical solution was obtained. The problem posed above is one of an inhomogeneous medium—of a discontinuous D as a function of x, or of a discontinuous Pe as a function of z. A Crank-Nicholson formulation for inhomogeneous media (Davis, 1984) was used to solve these equations. Again, values of $C_B = 0.5$ and $\kappa = 4.0$ have been used as representative values, and for comparison to the steady-state solutions above.

The transient concentration profile for $Pe_1 = 0.1$ with $Pe_2 = 10.0$ is illustrated in Figure 4. In region 1, the profiles

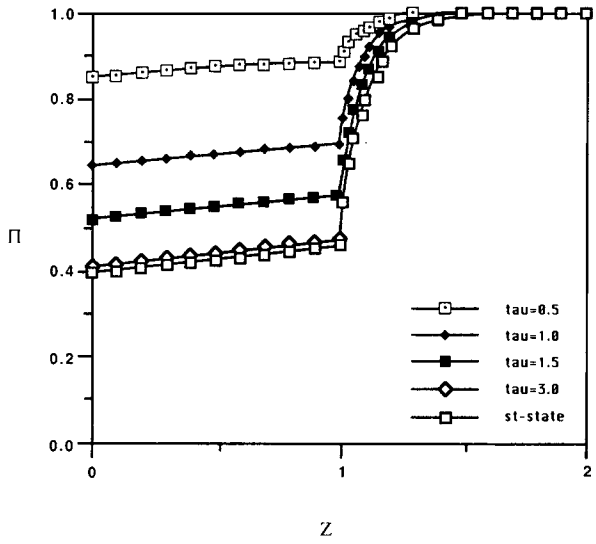

Figure 4. Transient profiles for $Pe_1 = 0.1$ and $Pe_2 = 10.0$.
$C_B = 0.5$ and $\kappa = 4.0$.

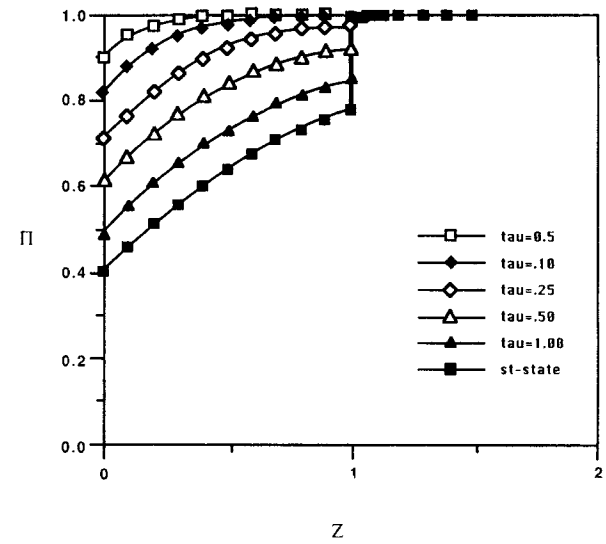

Figure 6. Transient profiles for $Pe_1 = 1.0$ and $Pe_2 = 100$.
$C_B = 0.5$ and $\kappa = 4.0$.

are relatively flat and concave down, characteristic of a low Pe_1. At the diffusion interface, the gradient is discontinuous, as previously demonstrated for the steady-state case. In region 2, the profiles increase sharply at first and then asymptotically approach C_B. Initially, the profile is flat at $\pi = 1$. As time increases, the curve shifts to overall lower values because of preferential sputtering at the surface. For $\tau = vt/\lambda = 3.0$, the profile has almost reached this steady-state profile. For $\tau > 30$, the transient profile is indistinguishable from the steady-state solution.

The transient concentration profiles for $Pe_1 = 1.0$ and for $Pe_2 = 10.0$ and $Pe_2 = 100.0$ are found in Figures 5 and 6, respectively. In region 1, the profiles are moderately increasing and concave down, characteristic of an intermediate Pe_1. At the interface the gradient is discontinuous, as previously observed for the steady-state case. In region 2, the profiles increase sharply at first and then asymptotically approach unity. The sharp increase at the entrance of region 2 in Figure 5 is less acute than the sharp increase at the entrance of region 2 in Figure 6, as expected. The steady-state solutions obtained above for the corresponding Pe_j are also plotted here.

The transient concentration profiles for $Pe_1 = 10.0$ and for $Pe_2 > 10.0$ are found in Figure 7. In region 1, the profiles increase very sharply and approach unity asymptotically, characteristic of a high value of Pe. At the interface the gradient is not discontinuous since the bulk concentration has already been reached, as observed for the corresponding steady-state curve. The time required to reach steady state was also much shorter, in this case for $\tau \geq 0.30$, the profile was almost indistinguishable from the steady-state curve.

From the figures presented above, the following can be inferred. The shape of the profile in region 1 is not influenced by the value of Pe_2 for $Pe_2 > Pe_1$. The depletion of component P is greater in the altered layer than in the unaltered bulk. As

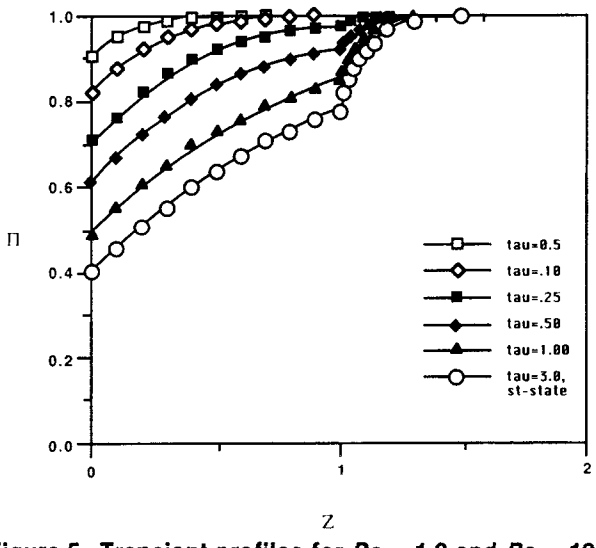

Figure 5. Transient profiles for $Pe_1 = 1.0$ and $Pe_2 = 10.0$.
$C_B = 0.5$ and $\kappa = 4.0$.

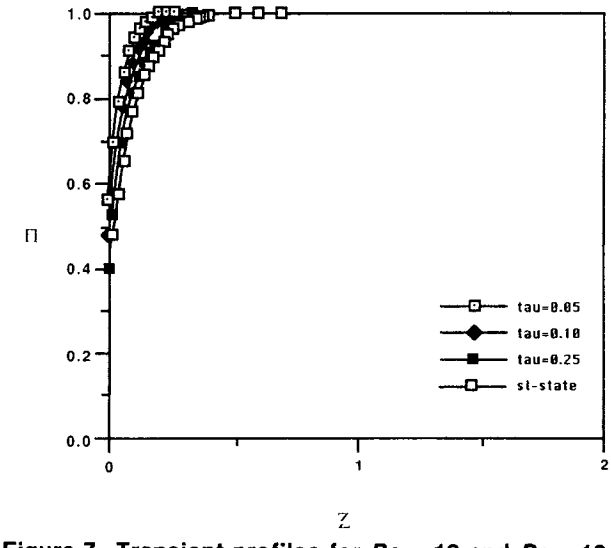

Figure 7. Transient profiles for $Pe_1 = 10$ and $Pe_2 \geq 10.0$.
$C_B = 0.5$ and $\kappa = 4.0$.

$Pe_2 \rightarrow Pe_1$, the discontinuity in gradient at the diffusion interface decreases. The greater Pe_2 is, the less the distance beyond the interface required for the concentration to reach its bulk value at any given τ. All of these observations also hold for the steady-state case. Finally, steady state is reached at approximately

$$\tau_{SS} \approx \frac{3.0}{Pe_1} \tag{38}$$

for $C_B = 0.5$ and $\kappa = 4.0$.

Summary

Previous models of competitive ion beam etching and mixing of solid surfaces consider an "altered layer" of indeterminate thickness as the mixing zone. The present model explicitly incorporates the penetration depth of the incident ions and assumes that the bulk diffusivities are unperturbed at greater depths. Its principal contributions are the introduction of the concept of the Peclet number to describe the ratio of rates of etching and mixing and the recognition that the Danckwerts boundary conditions apply at the interface between the region of radiation-enhanced mixing and the bulk. Both steady-state and transient concentration profiles have been presented for ion bombardment of semi-infinite binary alloys, under conditions where one component is more easily removed from the surface. The extension of this model to etching of thin films and its implications for typical methods of surface concentration analysis will be considered in future communications.

Acknowledgment

We gratefully acknowledge the support of the National Science Foundation (Grant CBT 84-51055) for this research.

Notation

C = mole fraction
C_B = mole fraction in semi-infinite bulk
C_δ = mole fraction in film
$C_{S,i}$ = mole fraction of i at the surface
$C_{S,SS}$ = mole fraction of easy-to-sputter component at surface at steady state
D = diffusivity
H = kinetic factor accounting for preferential sputtering
k_j = first-order rate constant for sputtering i
N_j = moles of component i
Pe_j = Peclet number in region j
S_i = sputter yield of component i
T = normalized time, Eq. 5
t = time
u = rate of surface recession
u_p = sputtering rate for P
v = negative of the rate of surface recession
X = normalized distance, Eq. 4
x = distance beneath the surface
z = dimensionless distance

Greek letters

β = enhancement factor for radiation-enhanced diffusion
δ = film thickness
κ = ratio of sputtering rate constants
λ = ion penetration depth
π = mole fraction normalized by initial bulk composition
ρ = molar density of the solid
τ = dimensionless time

Literature Cited

Betz, G., and G. K. Wehner, "Sputtering of Multicomponent Materials," in *Sputtering by Particle Bombardment II*, R. Behrisch, ed., Springer, Berlin, p. 11 (1983).
Birchenall, C. E., *Physical Metallurgy*, McGraw-Hill, New York (1959).
Bischoff, K. B., "A Note on the Boundary Conditions for Flow Reactors," *Chemical Eng. Sci.*, **16**, 131 (1961).
Borg, R. J., and G. J. Dienes, *An Introduction to Solid State Diffusion*, Academic Press, New York, p. 250 (1988).
Danckwerts, P. V., "Continuous Flow Systems: Distribution of Residence Times," *Chem. Eng. Sci.*, **2**, 1 (1953).
Davies, J. A., "Fundamental Concepts of Ion-Solid Interactions: Single Ions, 10^{-12} Seconds," *MRS Bull.*, **17**, 26 (1992).
Davies, M. E., *Numerical Methods and Modeling for Chemical Engineers*, John Wiley & Sons, New York (1984).
Elias, R. J., "The Effects of Enhanced Diffusion in Preferential Sputtering of Binary Alloys," M.ChE. thesis, University of Delaware (1990).
Gillam, E., "The Penetration of Positive Ions of Low Energy into Alloys and Composition Changes Produced by Them in Sputtering," *J. Phys. Chem. Solids*, **11**, 55 (1959).
Girifalco, L. A., *Atomic Migration in Crystals*, Blaisdell, New York (1964).
Ho, P. S., "Effects of Enhanced Diffusion on Preferred Sputtering of Homogeneous Alloy Surfaces," *Surface Sci.*, **72**, 253 (1978).
Ho, P. S., J. E. Lewis, H. S. Wildman, and J. K. Howard, "Auger Study of Preferred Sputtering of Binary Alloy Surfaces," *Surface Sci.*, **57**, 393 (1976).
Laegried, N., and G. K. Wehner, "Sputtering Yields of Metals for Ar^+ and Ne^+ Ions with Energies from 50 to 600 eV," *J. Appl. Phys.*, **32**, 365 (1961).
MacDonald, R. J., and D. Haneman, "Depths of Low-Energy Ion Bombardment Damage in Germanium," *J. Appl. Phys.*, **37**, 1609 (1966).
Mintz, M. H., Y. Jo, and J. W. Rabalais, "Thermalization-Reaction-Capture Model for Low Dose Active Ion Bombardment. II. Fast Diffusion Case," *J. Chem. Phys.*, **82**, 1275 (1985).
Ossi, P. M., "Ion-Beam-Induced Amorphization," *Materials Sci. and Eng.*, **90**, 55 (1987).
Pearson, J. R. A., "A Note on the Danckwerts' Boundary Conditions for Continuous Flow Reactors," *Chem. Eng. Sci.*, **10**, 281 (1959).
Peng, X. D., D. S. Edwards, and M. A. Barteau, "Formation of Magnesium Nitride Layers on the Mg(0001) Surface by Ion Implantation," *Surface Sci.*, **185**, 227 (1987).
Pickering, H. W., "Ion Sputtering of Alloys," *J. Vac. Sci. Technol.*, **13**, 618 (1976).
Picraux, S. T., E. Chason, and T. M. Mayer, "Ion-Assisted Surface Processing of Electronic Materials," *MRS Bull.*, **17**, 52 (1992).
Quinto, D. T., V. S. Sundaram, and W. D. Robertson, "Auger Spectra of Copper-Nickel Alloys," *Surf. Sci.*, **28**, 504 (1971).
Ryssel, H., and I. Ruge, *Ion Implantation*, John Wiley & Sons, New York (1986).
Schiøtt, H., "Approximations and Interpolation Rules for Ranges and Range Stragglings," *Radiation Effects*, **6**, 107 (1970).
Swartzfager, D. G., S. B. Ziemecki, and M. J. Kelley, "Differential Sputtering and Surface Segregation: The Role of Enhanced Diffusion," *J. Vac. Sci. Technol.*, **19**, 185 (1982).
Tarng, M. L., and G. K. Wehner, "Alloy Sputtering Studies with *in situ* Auger Electron Spectroscopy," *J. Appl. Phys.*, **42**, 2449 (1971).
Thornton, J. A., "Coating Deposition by Sputtering," in *Deposition for Films and Coatings*, R. F. Bunshah et al., eds., Noyes, New Jersey, p. 170 (1982).
van Cauwenberghe, A. R., "Further Note on Danckwerts' Boundary Conditions for Flow Reactors," *Chem. Eng. Sci.*, **21**, 203 (1966).
Wehner, J. F., and R. H. Wilhelm, "Boundary Conditions of Flow Reactor," *Chem. Eng. Sci.*, **6**, 89 (1956).
Williams, J. S., and M. M. Poate, *Ion Implantation and Beam Processing*, Academic Press, Australia (1984).

Manuscript received Feb. 11, 1992, and revision received July 23, 1992.